

3.2 Kinetics of Oxide Growth of Passive Films on Transition Metals

Katie Lutton, John R. Scully

Center for Electrochemical Science and Engineering
 Department of Materials Science and Engineering
 University of Virginia, Charlottesville, VA, United States

Glossary

Symbol	Explanation (units)
a	PDM film growth constant (nm s^{-1})
A	CM film growth constant (nm^{-1})
A'	GGM film growth constant (m^3)
b	PDM film growth constant (nm^{-1})
B	CM film growth constant (nm^{-1})
c	PDM film growth constant (A cm^{-2})
C	FM film growth constant (nm)
C'	FM film growth constant (C cm^{-2})
C''	FM film growth constant (s^{-2})
C_m^M	concentration of element M in the alloy, m (m^{-3})
D	FM film growth constant (nm^{-1})
E	electric field strength (V m^{-1})
F	Faraday's constant ($96,487 \text{ C mol}^{-1}$)
k	parabolic oxidation rate constant for Wagner thick films ($\text{nm}^2 \text{ s}^{-1}$)
K	PDM film growth constant (nm^{-1})
M_{ox}	Oxide molar mass (g mol^{-1})
N_v	Avogadro's number ($6.02 \times 10^{23} \text{ atom mol}^{-1}$)
P	GGM film growth constant ($\text{m}^2 \text{ s}^{-1}$)
Q	GGM film growth constant ($\text{m}^2 \text{ s}^{-1}$)
q_{ox}	oxide charge density (C cm^{-2})
t	time (s)
V	film growth overpotential (V)
V_{app}	applied anodic potential (V)
x	oxide film thickness (nm)
x_d	Debye length (m)
$x_{t=0}$	initial oxide film thickness at $t = 0 \text{ s}$ (nm)
z	cation valency (eq mol^{-1})

Ω	oxide molar volume (mol cm^{-3})
$\Phi_{\text{m/f}}^{\text{ns}}$	nonsteady-state metal/film interfacial potential drop (V)
$\Phi_{\text{m/f}}^{\text{ss}}$	steady-state metal/film interfacial potential drop (V)
$\Phi_{\text{f}}^{\text{ns}}$	nonsteady-state passive film potential drop (V)
$\Phi_{\text{f}}^{\text{ss}}$	steady-state passive film potential drop (V)
$\Phi_{\text{f/s}}^{\text{ns}}$	nonsteady-state film/solution interfacial potential drop (V)
$\Phi_{\text{f/s}}^{\text{ss}}$	steady-state film/solution interfacial potential drop (V)
ρ_{ox}	oxide density (g cm^{-3})

Abstract

The objective of this chapter is to summarize the oxide growth mechanisms and rate controlling processes for typical transition metals such as Fe, Cr, and Ni in aqueous solutions. Kinetic expressions and mechanisms for oxide growth at potentials in the passive range as defined in section 3.1 are described based on the Mott-Cabrera, Fehlnert-Mott, Point Defect, and the Generalized Growth models. It is shown that oxide growth can be controlled by either the metal cation ejection rate at the metal/film interface, the transport kinetics of defects as charge carriers across the passive film, or the metal cation dissolution rate at the oxide/solution interface. Thin passive films ($x < 10\text{-}20$ nm) may exhibit direct logarithmic, inverse logarithmic, parabolic, or linear growth with respect to time depending on which model is applied while thick films grow by parabolic kinetics.

Keywords: passive films, oxide growth, Cabrera-Mott model, Fehlnert-Mott model, Point Defect model, Generalized Growth model, oxide film, ionic defects, electronic defects, logarithmic growth law, parabolic growth rate law

1. Introduction

Oxides provide kinetic protection to a number of metals and alloys in harsh environments, serve as functional materials in electronic applications, provide color stability in optical and architectural applications, and produce bio-compatible surfaces to promote biological interface stability. Oxide films serve to reduce the corrosion rate of otherwise active metals in harsh environments. These functions are dependent on the identity, thickness, defect type, concentration, and mobility of charge carriers, their subsequent transport, electronic properties, and the relevant driving force for oxide formation. These factors collectively determine the 'corrosion rate' of a passive metal, often defined as the quasi-steady state passive current density assuming the oxide does not rupture, spall, or delaminate nor breakdown chemically. Hence film thickness, identity, composition, crystalline defects, and electronic properties, amongst other parameters, are crucial. Establishment of the kinetics of oxide growth, steady-state oxide thickness, or a limiting oxide thickness are topics of high interest. In many cases the oxide grows either by an inverse logarithmic or logarithmic law (thin films, $x < 10\text{-}20$ nm) or parabolic growth laws ($x > 1$ μm) with respect to time. However, the details of these growth rate laws depend

critically on the assumed mechanisms and conditions. The rates and controlling factors depend on the crystal structure of the underlying metal, epitaxy and misfit of the oxide on the metal, predominant ionic and electronic defects responsible for field-assisted charge transport, transport processes across the oxide film, and the controlling processes at the metal/film and the film/solution interfaces.

In all of the models presented, the driving force consisting of the applied voltage is divided into the electric field gradient across the oxide, the potential at the oxide/metal, and film/solution interfaces [1–3] as shown schematically in Figure 1. The oxide growth behavior is a complex process of the rate controlling processes at each interface and across the film subjected to the driving forces applied at these positions. In some models, the potentials shown in Figure 1 do not change with oxide thickness while in others they are modified as detailed below. The objective of this section is to highlight some of these controlling factors and convey how they affect growth rate behavior.

<Figure 1 near here>

2. Factors Controlling Film Growth in the Passive region

Growth as a Function of Time

The development of oxide growth models originates from Wagner’s original assumption that metal oxidation proceeds by diffusion of charged particles and has been well-validated for thick film growth ($x > 1 \mu\text{m}$) typical for passive metals exposed to high temperatures [4]. By invoking a linear diffusion equation which incorporated the electric field across semiconducting passive oxides, Wagner found that film growth is parabolic:

$$x = (kt)^{1/2} \quad (1)$$

where x is the film thickness, k is the parabolic rate constant, and t is time. From this solution, Cabrera and Mott developed the high field approach to solve for thin film growth where a high electric field is maintained and assists the diffusion of ionic point defects necessary for oxidation reactions. Cabrera and Mott hypothesized in 1949 that thin film growth was directly dependent on the migration of interstitial cations where the rate limiting step is cation injection at the metal/film interface [5]. The assumed uniform electric field triggers a shift in the Fermi level across the film, also called the Mott potential, which drives ionic transport and electron tunnelling. Cabrera and Mott’s solution for thin film growth at low temperatures yields an inverse logarithmic growth law [5]:

$$\frac{1}{x} = A - B \ln t \quad (2)$$

where A and B are high field growth constants. The C-M model can be extended to films thicker than several nanometers by assuming electron transport occurs via thermionic emission or by typical semiconductor processes across an oxide, yielding parabolic growth kinetics seen by Wagner [4].

Following the C-M model, Mott and Fehlnner published an evolution on the previous model which was developed using similar assumptions [6]. Their solution invoked the assumption that transport of

interstitial anions, rather than cations, across the film is assisted by the electric field and acted as the rate limiting step. Their derivation yields direct logarithmic growth [6]:

$$x = C \ln(1 + Dt) \quad (3)$$

where C and D are growth constants dependent on the oxide structure. Unlike C-M, the F-M model assumes the electric field is constant with film thickness growth. As the field is approximated as:

$$E = \frac{V_{app}}{x} \quad (4)$$

where V_{app} is the applied potential for anodic film growth, Eq. 4 cannot be constant with film growth as V_{app} is typically constant while x is changing. The proposed mechanism for growth, migration of anions via interstitial sites, is also unrealistic of physical processes due to steric hindrance in a typical crystalline oxide with a close-packed structure. These limitations yield an inappropriate description of electrochemical film growth; hence F-M is not commonly applied for analysis of film growth kinetics. Additionally, both the C-M and F-M models were developed for dry oxidation as the impact of aqueous solutions and the possibility of dissolution reactions were not considered [2].

The broad assumptions inherent in the C-M and F-M models were addressed in 1981 by MacDonald's Point Defect Model (PDM). There, both cation and anion point defect transport control the growth and dissolution of anodic passive films [7]. Macdonald's solution applies to thin films where growth is limited by either interfacial anion injection or oxygen vacancy transport [7,8]. The model applies very well to electrochemical film growth as it takes into account interfacial potential drops, which are functions of the solution pH and applied anodic potential, and film dissolution by a chemical process. The PDM yields direct logarithmic growth laws for both interfacial-controlled [8] and transport-controlled processes [7] as indicated in Figure 2. The PDM solution for interface-controlled film growth is given as:

$$x = x_{t=0} + \frac{1}{b} \ln[1 + abt \exp(-bx_{t=0})] \quad (5)$$

whereas film growth controlled by defect transport is given as:

$$x = \frac{1}{2K} [\ln 2Ka(b - 1) + \ln t] \quad (6)$$

where a, b, and K are constants and $x_{t=0}$ is the initial film thickness. A major limitation of the PDM is that it does not account for unsteady film growth before a limiting thickness is reached. This is due to the time-dependence of the electric field strength and potential drops at film interfaces during transient film growth and their influence on reaction kinetics. Additionally, the model inappropriately includes dependence of the metal/film interfacial potential drop on the solution pH while instead it should be dictated by the epitaxy of the metal substrate with the oxide film.

<Figure 2 near here>

The Generalized Growth Model (GGM) was published in order to analyze the kinetics of non-stationary electrochemical film growth where typical quasi-steady-state approximations present in the C-M, F-M, and PDM are not applicable [2]. Their mathematical solution included the metal/film interfacial epitaxy and its relevant potential drop, along with time and solution-dependence of the film/solution interfacial potential drop for accurate analysis of film growth controlled by either charged species transport or cation ejection at the metal/film interface. Film chemical dissolution reactions in aqueous environments are included as they lead to the occurrence of steady-state thicknesses balanced by the oxidation current density. The time-dependence of film growth by the GGM yields a linear relationship for interface-controlled film growth reactions given as:

$$x = A' C_m^M t \quad (7)$$

whereas transport-controlled film growth yields a parabolic relationship:

$$x = \sqrt{(P + Q)t} \quad (8)$$

where A' , P , and Q are constants derived in the model solution and C_m^M is the concentration of element M in the metal alloy, m . The model additionally notes that growth controlled by cation injection at the metal/oxide interface will only occur when given strong electric fields present for ultrathin films ($x < 2$ nm), thus it is relevant for early stages of passivation. The crucial information invoked in the GGM, along with the C-M, F-M and PDM are summarized in Table 1.

<Table 1 near here>

Further analysis of growth kinetics can be found using current transients. The expression for the current density contribution to film growth is given by Faraday's law:

$$i_{ox}(t) = \frac{zF\rho_{ox}}{M_{ox}} \frac{dx}{dt} \quad (9)$$

where z is the cation valency, F is Faraday's constant, ρ_{ox} is the oxide density, and M_{ox} is the molar mass of the oxide. The expression can be applied to the film growth relationships proposed by the aforementioned models. This yields the following expressions for the oxidation current density, i_{ox} , and their transients shown in Table 2:

<Table 2 near here>

There exists another new model in literature, the Mass Charge Balance model, which demonstrates accurately simulates of transient potentiostatic passivation on pure Fe, Co-Cr, and Fe-Ni-Cr alloys [17]. The MCB provides a solution for alloy oxidation and dissolution rates as a function of electrode potential, pH, and temperature by considering elementary electrochemical redox reactions and unsteady potential drops at the interfaces shown in Figure 1 along with charged defect transport across the film. The model is not included in Tables 1 and 2 because it yields approximately the same growth law as the PDM (Eq. 6). Additionally, the model provides for numerical predictions of passivation data, rather than an exact solution of x and i_{ox} .

A final and commonly used metric for film growth kinetics involves application of the following equation for high field anodic film growth [9]:

$$i_{ox}(t) = A \exp\left(\frac{BV}{q_{ox}(t)}\right) \quad (10)$$

or by rearranging,

$$\log i_{ox}(t) = \log A + 2.303 \frac{BV}{q_{ox}(t)} \quad (11)$$

These expressions are valid when:

$$q_{ox}(t) = \int_0^t i_{ox}(t) dt \quad (12)$$

and the overpotential for film growth is given as:

$$V = V_{app} - E_{pp} \quad (13)$$

where q_{ox} is the oxide charge density and E_{pp} is the critical potential for passive film growth. Construction of a plot for q_{ox}^{-1} versus $\log i_{ox}$ enables graphical analysis of the high field growth constants, A and B, from the linear region. As film thickening, rather than nucleation or coalescence of oxide particles, occurs at higher time and, thus, charge, the relevant region for model application will be at low q_{ox}^{-1} and i_{ox} . The high field constants directly control film growth according to Eq. 10 as increasing A and B causes an increase in i_{ox} and thus q_{ox} and film thickness, x , as they are derived from its integral.

Analysis of both the high field parameters and current transients can yield crucial information on the validity of the various oxidation models presented in literature. Depending on the given metal or alloy and the aqueous environment, analysis of film growth data will indicate which model is applicable and provide insight into what the controlling reactions may be.

Growth as a Function of Applied Potential

A common feature observed in many metals is that the quasi-stationary passive current density at a given applied potential reaches an approximate steady state value which is approximately potential independent (Section 3.1). In original formulations, this was because cation dissolution at the film/solution interface depended on the oxide structure, cation concentration, activation energy for metal cation dissolution, and pH whereas the potential drop at the oxide/solution interface depended only on pH [7,18]. Thus, these conditions did not change with potential. Later models argued that this interfacial potential varies slightly with applied voltage [2]. In stationary conditions the dissolution rate is balanced by the oxide film growth rate. Moreover, the stationary limiting film thickness increases linearly with applied potential. These two observations make sense in the context of the growth models discussed in Section 2.1 in that the field across the oxide might remain constant if an increase in applied voltage yielded a commensurate increase in stationary film thickness (Eq. 4). These are taken to imply that an oxide formation rate equivalent to the oxide dissolution rate at each applied potential where a linearly increasing steady state oxide thickness with linearly increasing potential yields the same field strength at each potential, provided the potential is distributed across the oxide. In any case, many

transition metals possess such a linear relationship between oxide thickness and applied potential in the passive range. This is often observed, albeit the relationship $\frac{\partial x}{\partial E}$ varies with material, solution, and electrochemical conditions.

There exists another recent solution for film growth in literature, the Mixed Conduction Model, but unlike the previous models it does not consider transient film growth [19–21]. Rather, the model addresses steady-state passive films and the potential-dependence of layer thickness which results from coupling ionic defect structures with electronic conduction [19]. As such, the Mixed Conduction Model is not included in Tables 1 and 2.

3. Summary

Kinetic expressions and mechanisms for the kinetics of oxide growth at potentials in the passive range as defined in Section 3.1 are described by the Mott-Cabrera, Fehlner-Mott, Point Defect and the Generalized Oxide Growth Models. It is shown that oxide growth can be controlled by either metal cation ejection rate at the metal/film interface, transport kinetics of defects across the passive film, or metal cation dissolution at the oxide/solution interface. A major factor which remains unclear is how the applied potential is distributed across the oxide and its interfaces and a challenge remains to accurately define the rate controlling process which accounts for all material, electrochemical and environmental variables. Nevertheless, the thickness of thin passive films ($x < 10\text{-}20$ nm) under transport-controlled conditions was historically found to follow inverse logarithmic or logarithmic growth laws, although the Generalized Growth model yielded parabolic oxide growth kinetics. Under thick film conditions, the Wagner law is usually observed.

4. Embedded Tables, Figures, and Captions

Table 1. Summary of the Cabrera-Mott, Fehlner-Mott, Point Defect, and Generalized Growth Models. Adapted from [2].

	Cabrera-Mott model (gas phase formation) [5,9–11]	Fehlner-Mott model (gas phase formation) [6,12]	Point Defect Model (electrochemical formation) [7,13–15]	Generalized Growth Model (electrochemical formation) [2,16]
Oxide Growth Mechanism	Migration of interstitial cations	Migration of interstitial anions	Migration of anion vacancies	Migration of charged species
Growth Law	Weak Electric Field: $x^2 = Et$ Strong Electric Field: $\frac{1}{x} = A - B \ln t$	Activation energy function of thickness $x = C \ln(1 + Dt)$	Transport Controlled: $x = \frac{1}{2K} [\ln 2Ka(b - 1) + \ln t]$ Interface Controlled: $x = x_{t=0} + \frac{1}{b} \ln[1 + abt \exp(-bx_{t=0})]$	Transport Controlled: $x = \sqrt{(P + Q)t}$ Interface Controlled: $x = A' C_m^M t$
Limiting Growth Step	Weak Electric Field: Transport of cations through the film Strong Electric Field: Cation injection at m/f interface	Anion transport through the film	Transport Controlled: Oxygen vacancies through film Interface Controlled: Anion vacancy injection at m/f interface	Transport Controlled: Cation and anion transport through film via interstitials and vacancies Interface Controlled: Cation injection at m/f interface
Electric Field	$E = \frac{V}{x}$	Independent of x	Independent of x	Constant (linear potential gradient)
Dissolution	n/a	n/a	Dissolution of metal Dissolution of oxide	Unsteady dissolution of oxide dependent of film structure
Crystalline Defects in Oxide Layer (Grain Boundaries)	No	Modification of the growth law (grain boundaries)	No	Structure contribution included in model
Interfacial potential drop	No	No	Yes, function of pH and V_{ext}	Yes, constant at m/f interface and unsteady at f/s interface until limiting x reached

Table 2. Oxidation current densities and corresponding logarithmic transient solutions according to the Cabrera-Mott, Fehlner-Mott, Point Defect, and Generalized Growth models.

Model	$i_{ox}(t)$	$\frac{\partial \log i_{ox}(t)}{\partial \log t}$
Cabrera-Mott [9]	$\frac{BV}{t \left[\ln \left(\frac{i_{ox}}{A} \right) \right]^2}$	$-\frac{\ln \left(\frac{i_{ox}}{A} \right)}{2 + \ln \left(\frac{i_{ox}}{A} \right)}$
Fehlner-Mott [6]	$\frac{C'D}{1 + Dt}$	$-\frac{t}{C'D(Dt + 1)}$
Point Defect [7]	Transport Controlled: $\frac{FN_v}{K\Omega} t^{-1}$ Interface Controlled: $\frac{c}{abt + \exp(-bx_{t=0})}$	Transport Controlled: $^{-1}$ Interface Controlled: $\frac{ab}{abt^2 + t \exp(-bx_{t=0})}$
Generalized Growth [2]	Transport Controlled: $\frac{P + Q \exp \left[-\sqrt{\frac{(P+Q)t}{x_d}} \right]}{\sqrt{(P+Q)t}}$ Interface Controlled: $A' C_m^M$	Transport Controlled: $-\frac{1}{2} \left[1 + \sqrt{\frac{(P+Q)}{x_d}} t \left(\frac{Q \exp \left[-\sqrt{\frac{(P+Q)t}{x_d}} \right]}{P + Q \exp \left[-\sqrt{\frac{(P+Q)t}{x_d}} \right]} \right) \right]$ Interface Controlled: 0

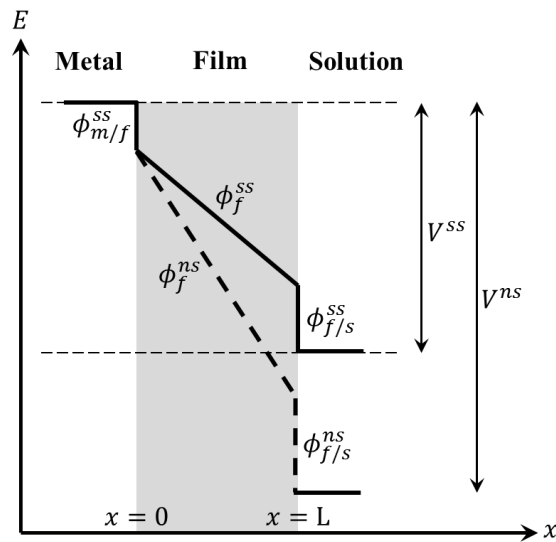


Figure 1. Potential drops across the metal/film/solution interfaces for non-steady and steady-state growth conditions, shown with dashed and solid lines, respectively.

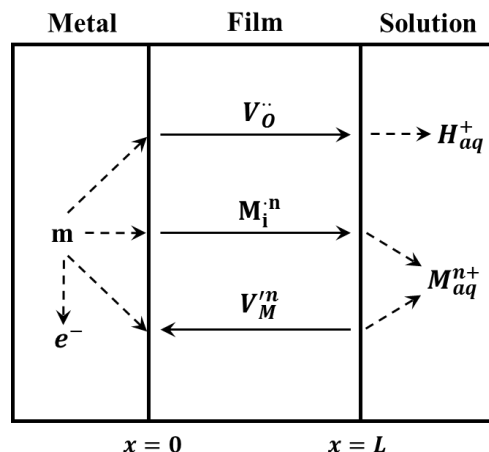


Figure 2. Kroger-Vink point defects relevant for Point Defect Model analysis of transport and growth mechanisms where the solid lines indicate defect transport and dashed ones indicate chemical reactions

5. References

- [1] M. Momeni, M. Behazin, J.C. Wren, Mass and Charge Balance (MCB) Model Simulations of Current, Oxide Growth and Dissolution during Corrosion of Co-Cr Alloy Stellite-6, *J. Electrochem. Soc.* 163 (2015) C94–C105. doi:10.1149/2.0721603jes.
- [2] A. Seyeux, V. Maurice, P. Marcus, Oxide Film Growth Kinetics on Metals and Alloys: I. Physical Model, *J. Electrochem. Soc.* 160 (2013) C189–C196. doi:10.1149/2.036306jes.
- [3] Z. Xu, K.M. Rosso, S. Brummer, Metal oxidation kinetics and the transition from thin to thick films, *Phys. Chem. Chem. Phys.* 14 (2012) 14534–14539. doi:10.1039/c2cp42760e.
- [4] A.T. Fromhold, *Theory of Metal Oxidation*, North Holland Publishing Company, Amsterdam, 1976.
- [5] N. Cabrera, N.F. Mott, *Theory of the oxidation of metals*, *Reports Prog. Phys.* 12 (1949) 163–184. doi:10.1088/0034-4885/12/1/308.
- [6] F.P. Fehlner, N.F. Mott, Low-temperature oxidation, *Oxid. Met.* 2 (1970) 59–99. doi:10.1007/BF00603582.
- [7] C.Y. Chao, L.F. Lin, D.D. Macdonald, A point defect model for anodic passive films I. Film growth kinetics, *J. Electrochem. Soc.* 128 (1981) 1187–1194. doi:10.1149/1.2127591.
- [8] D. Macdonald, S. Biaggio, H. Song, Steady State Passive Films Interfacial Kinetic Effects and Diagnostic Criteria, *J. Electrochem. Soc.* 139 (1992) 170–177. doi:10.1149/1.2069165.
- [9] G.T. Burstein, A.J. Davenport, The Current-Time Relationship during Anodic Oxide Film Growth under High Electric Field, *J. Electrochem. Soc.* 136 (1989) 936–941. doi:10.1149/1.2096890.
- [10] A.J. Davenport, G.T. Burstein, Concerning the Distribution of the Overpotential during Anodic Oxide Film Growth, *J. Electrochem. Soc.* 137 (1990) 1496–1501.
- [11] A.J. Davenport, B.K. Lee, Passive Film Growth Kinetics for Iron and Stainless Steel, *Electrochem. Soc. Proc.* 13 (2002) 187–197.
- [12] F.P. Fehlner, Low temperature oxidation of metals and semiconductors, *J. Electrochem. Soc.* 131 (1984) 1645–1652.
- [13] L.F. Lin, C.Y. Chao, D.D. Macdonald, A point defect model for anodic passive films II. Chemical breakdown and pit initiation, *J. Electrochem. Soc.* 128 (1981) 1194–1198. doi:10.1149/1.2127592.
- [14] C.Y. Chao, L.F. Lin, D.D. Macdonald, A point defect model for anodic passive films III. Impedance response, *J. Electrochem. Soc.* 129 (1982) 1874–1879. doi:10.1149/1.2124318.
- [15] D.D. Macdonald, The Point Defect Model for the Passive State, *J. Electrochem. Soc.* 139 (1992) 3434–3449. doi:10.1149/1.2069096.
- [16] K. Leistner, C. Toulemonde, B. Diawara, A. Seyeux, V. Maurice, P. Marcus, Oxide Film Growth Kinetics on Metals and Alloys: II. Numerical Simulation of Transient Behavior, *J. Electrochem. Soc.* 160 (2013) C197–

- C205. doi:10.1149/2.036306jes.
- [17] M. Momeni, J.C. Wren, A Mechanistic Model for Oxide Growth and Dissolution during Corrosion of Cr-Containing Alloys, *Faraday Discuss.* 180 (2015) 1–23. doi:10.1039/C4FD00244J.
 - [18] H. Kaesche, *Corrosion of Metals: Physicochemical Principles and Current Problems*, 1st ed., Springer-Verlag, Berlin, 2003. doi:10.1007/978-3-642-96038-3.
 - [19] M. Bojinov, G. Fabricius, T. Laitinen, K. Mäkelä, T. Saario, G. Sundholm, Coupling between ionic defect structure and electronic conduction in passive films on iron, chromium and iron-chromium alloys, *Electrochim. Acta.* 45 (2000) 2029–2048. doi:10.1016/S0013-4686(99)00423-5.
 - [20] M. Bojinov, G. Fabricius, T. Laitinen, K. Mäkelä, T. Saario, G. Sundholm, Influence of molybdenum on the conduction mechanism in passive films on iron-chromium alloys in sulphuric acid solution, *Electrochim. Acta.* 46 (2001) 1339–1358. doi:10.1016/S0013-4686(00)00713-1.
 - [21] B. Beverskog, M. Bojinov, P. Kinnunen, T. Laitinen, K. Mäkelä, T. Saario, A mixed-conduction model for oxide films on Fe, Cr and Fe-Cr alloys in high-temperature aqueous electrolytes - II. Adaptation and justification of the model, *Corros. Sci.* 44 (2002) 1923–1940. doi:10.1016/S0010-938X(02)00009-4.

6. Further Reading

Books

- Chiang, Y., Birnie, D., & Kingery, W. D. (1997). *Physical ceramics: Principles for ceramic science and engineering*. John Wiley & Sons, Inc.
- Jones, D. A. (1992). *Principles and prevention of corrosion*. Macmillan.
- Marcus, P. (2011). *Corrosion mechanisms in theory and practice*. CRC Press.
- McCafferty, E. (2010). *Introduction to corrosion science*. Springer.
- Young, D. J. (2016). *High temperature oxidation and corrosion of metals*. Elsevier Science.

7. Cross References

Passivation and Stainless Steels and other Chromium Bearing Alloys, Corrosion, Surface Analysis, Titanium, Aluminum, Zirconium chapters